Biosensors and Bioelectronics 123 (2019) 114–123

Contents lists available at ScienceDirect

Biosensors and Bioelectronics

journal homepage: www.elsevier.com/locate/bios

Designer fungus FAD glucose dehydrogenase capable of direct electron transfer

Kohei Ito[a], Junko Okuda-Shimazaki[b], Kazushige Mori[b], Katsuhiro Kojima[b], Wakako Tsugawa[a], Kazunori Ikebukuro[a], Chi-En Lin[c], Jeffrey La Belle[c], Hiromi Yoshida[d], Koji Sode[a,b,e,*]

[a] Department of Biotechnology and Life Science, Graduate School of Engineering, Tokyo University of Agriculture and Technology, 2-24-16 Naka-cho, Koganei, Tokyo 184-8588, Japan
[b] Ultizyme International Ltd., 1-13-16, Minami, Meguro, Tokyo 152-0013, Japan
[c] School of Biological and Health System Engineering, Ira A. Fulton Schools of Engineering, Arizona State University, P.O. Box 879709, Tempe, AZ 85287-9719, USA
[d] Life Science Research Center and Faculty of Medicine, Kagawa University, 1750-1 Ikenobe, Miki-cho, Kita-gun, Kagawa 761-0793, Japan
[e] Joint Department of Biomedical Engineering, The University of North Carolina at Chapel Hill and North Carolina State University, Chapel Hill, NC 27599, USA

ARTICLE INFO

Keywords:
Glucose dehydrogenase
Cellobiose dehydrogenase
Direct electron transfer
Designer FADGDH
Fusion protein
Heme *b*-binding cytochrome domain

ABSTRACT

Fungi-derived flavin adenine dinucleotide glucose dehydrogenases (FADGDHs) are currently the most popular and advanced enzymes for self-monitoring of blood glucose sensors; however, the achievement of direct electron transfer (DET) with FADGDHs is difficult. In this study, a designer FADGDH was constructed by fusing *Aspergillus flavus* derived FADGDH (AfGDH) and a *Phanerochaete chrisosporium* CDH (PcCDH)-derived heme *b*-binding cytochrome domain to develop a novel FADGDH that is capable of direct electron transfer with an electrode. A structural prediction suggested that the heme in the CDH may exist in proximity to the FAD of AfGDH if the heme *b*-binding cytochrome domain is fused to the AfGDH N-terminal region. Spectroscopic observations of recombinantly produced designer FADGDH confirmed the intramolecular electron transfer between FAD and the heme. A decrease in pH and the presence of a divalent cation improved the intramolecular electron transfer. An enzyme electrode with the immobilized designer FADGDH showed an increase in current immediately after the addition of glucose in a glucose concentration-dependent manner, whereas those with wild-type AfGDH did not show an increase in current. Therefore, the designer FADGDH was confirmed to be a novel GDH that possesses electrode DET ability. The difference in the surface electrostatic potentials of AfGDH and the catalytic domain of PcCDH might be why their intramolecular electron transfer ability is inferior to that of CDH. These relevant and consistent findings provide us with a novel strategic approach for the improvement of the DET properties of designer FADGDH. (241 words)

1. Introduction

Diabetes mellitus is a serious modern disease worldwide. Monitoring of blood glucose by the patient, known as self-monitoring of blood glucose (SMBG), is an essential procedure for patients with diabetes mellitus to help control their glycemic levels. In addition, a continuous glucose monitoring (CGM) system is essential and is currently considered to be state of the art. A CGM system measures glucose levels in the interstitial fluid by inserting an enzyme sensor into the subcutaneous area. Recently, the U.S. Food and Drug Administration approved an artificial pancreas, consisting of a CGM system, a continuous subcutaneous insulin infusion pump, and control algorithms. Among the principles reported for electrochemical sensors to measure glucose using a variety of glucose oxidoreductases, the third-generation principle, employing the direct electron transfer (DET) principle, is considered to be the most elegant and ideal for use in CGM. Since the third-generation principle utilizes no electron mediator or oxygen, the use of toxic artificial electron mediators is not necessary, and errors due to variations in the concentration of oxygen in blood samples are eliminated. However, glucose oxidoreductases capable of DET are limited.

Fungi-derived flavin adenine dinucleotide glucose dehydrogenases (FADGDHs) are currently the most popular and advanced enzymes for SMBG sensors due to their superior substrate specificity and insensitivity to oxygen (Ferri et al., 2011). The first FADGDH, derived from *Aspergillus oryzae*, was reported decades ago (Bak, 1967a, 1967b;

* Corresponding author: Joint Department of Biomedical Engineering, The University of North Carolina at Chapel Hill and North Carolina State University, Chapel Hill, NC 27599, USA.
E-mail address: ksode@email.unc.edu (K. Sode).

https://doi.org/10.1016/j.bios.2018.07.027
Received 3 May 2018; Received in revised form 12 July 2018; Accepted 13 July 2018
Available online 26 July 2018
0956-5663/

Bak and Sato, 1967a, 1967b; Ogura and Nagahisa, 1937). The FADGDHs reported thus far have shown specific characteristics (Ozawa et al., 2017; Piumi et al., 2014; Satake et al., 2015; Sygmund et al., 2011a, 2011b; Tsujimura et al., 2006; Yang et al., 2014, 2015). An FADGDH from *Aspergillus flavus* (AfGDH) has also been reported (Mori et al., 2011), and its improvement of thermal stability was achieved by introducing an intramolecular disulfide bond (Sakai et al., 2015). The 3D structure of AfGDH was also elucidated (Yoshida et al., 2015), revealing that the redox cofactor FAD is buried deeply within the FADGDH protein molecule. The previous reports (Wilson, 2016; Bartlett and Al-Lolage, 2017) identified the voltammograms associated with GOx to be due to free FAD. The spectroelectrochemistry (Vogt et al., 2014) demonstrated that bound FAD exhibits electron transfer at a more positive potential not observed in voltammetry. Thus DET of GOX or fungi-derived FADGDH is difficult. Recently, we reported on a glucose sensor using mediator-modified FADGDH that was fabricated by a new method using the prefunctionalized amine reactive phenazine ethosulfate (arPES) (Hatada et al., 2018). This mediator-modified GDH showed the ability to transfer electrons to bulky electron acceptors, as well as to electrodes. In other words, the presence of an electron acceptor in proximity to FAD and the protein surface transforms FADGDH into a DET enzyme.

Extracellular fungal flavocytochrome cellobiose dehydrogenases (CDHs) are enzymes capable of DET activity. CDHs are composed of two domains: a heme *b*-binding cytochrome domain and a FAD-binding dehydrogenase catalytic domain which are connected by a flexible linker. Over the past two decades, these enzymes have been investigated for their mechanism of catalytic reaction (Desriani et al., 2010; Harreither et al., 2012; Sygmund et al., 2012), electron transfer ability (Kadek et al., 2015, 2017; Kracher et al., 2015) and unique structure (Hallberg et al., 2000, 2002). Recently, the overall crystal structures of CDHs derived from *Myriococcum thermophilum* and *Neurospora crassa* were elucidated (Tan et al., 2015). Their full-length crystal structures, together with the proposed conformational changes, show the ability of a flavin-to-heme interdomain electron transfer, which motivated us to design an engineered DET-type FADGDH, harboring the electron transfer domain of CDH.

In this study, the designer FADGDH was constructed using CDH structural information. AfGDH was selected as the catalytic domain and linked to a *Phanerochaete chrisosporium* CDH (PcCDH)-derived heme *b*-binding cytochrome domain with a native linker. The recombinant production of the designer FADGDH resulted in a soluble and active FADGDH, showing flavin-to-heme interdomain electron transfer during the oxidation of glucose. Most remarkably, this molecule showed DET ability to the electrode and maintained the original substrate specificity of FADGDH.

2. Materials and methods

2.1. Materials

Bacto™ yeast extract, yeast nitrogen base without amino acids and ammonium sulfate, and Bacto™ tryptone were obtained from BD Bioscience (San Jose, CA, USA). (+)-Biotin was obtained from Fujifilm Wako Pure Chemical Co. (Oosaka, Japan), Phenazine methosulfate (PMS), 2,6-dichlorophenolindophenol (DCIP) and 3-(4,5-Dimethyl-2-thiazolyl)-2,5-diphenyl-2H-tetrazolium bromide (MTT) were obtained from Kanto Chemical Co., Inc. (Tokyo, Japan) Disposable screen-printed carbon electrode (SPCE) strips with two carbon-plate electrodes and an Ag/AgCl electrode, DEP-Chip were obtained from Biodevice Technology (Ishikawa, Japan). All other chemicals were of reagent grade. Platinum (Pt) wire was purchased from TANAKA Kikinzoku (Tokyo, Japan). The silver/silver chloride (Ag/AgCl) reference electrode was purchased from BAS Inc. (Tokyo, Japan).

2.2. Design of engineered FADGDH and construction of expression vector

The 3D crystal structures of AfGDH (PDB:4YNU) (Yoshida et al., 2015), PcCDH flavin domain (PDB:1KDG) (Martin Hallberg et al., 2002) and full-length MtCDH (PDB:4QI6) (Tan et al., 2015) were referenced from The Research Collaboratory for Structural Bioinformatics Protein Data Bank. This information enabled us to develop the construct of the CDH heme *b*-binding domain linked with AfGDH as the catalytic domain. The PcCDH full-length structural gene was synthesized by Eurofins Genomics (Luxembourg, Belgium). The 5′-primer contained a SnaB1 restriction site, and the 3′-primer contained the AfGDH N-terminal sequence that was used for amplification of the heme *b*-binding domain structural gene. The 5′primer also contained a linker sequence, and the 3′-primer contained a Not1 restriction site, which was used for amplification of the AfGDH structural gene. The structural gene with a PcCDH native linker sequence without the original signal sequence was amplified from the purchased synthetic gene of the full-length PcCDH. The AfGDH structural gene without the original signal sequence was amplified by PCR from the previously engineered expression vector for *E. coli* (Mori et al., 2011). The N-terminal of AfGDH was then genetically linked with heme *b*-binding domain via the native linker sequence by using the overlap PCR method. The designed gene cassette was inserted into the multicloning site of expression vector pPIC9 (Thermo Fisher Scientific, Massachusetts, USA), in which the structural gene was under the control of the AOX1 promoter, and the α-factor signal sequence was used for secretion.

2.3. Expression and purification

The designed FADGDH expression vector was transformed into the *Pichia pastoris* strain KM71 using the LiCl integration method (Ito et al., 1983). The resulting plasmid was linearized by *Stu*I and transformed into competent cells. Screening of the transformants was performed on MGY agar plates (consisting of 0.34 % Yeast Nitrogen Base w/o amino acid and ammonium sulfate, 1 % ammonium sulfate, 1 % glycerol, 0.00004 % Biotin) and the clones were confirmed by a colony PCR kit (Promega, Wisconsin, USA). Five transformants were used for protein expression at the test tube scale to obtain the optimal clones, regarding enzyme activity. Each clone was inoculated into 3 mL of BMGY medium (consisting of 1 % Yeast extract, 2 % peptone, 100 mM Potassium phosphate buffer pH 6.0, 0.34 % Yeast Nitrogen Base w/o amino acid and ammonium sulfate, 1 % ammonium sulfate, 1 % glycerol, 0.00004 % Biotin) and incubated at 30 °C for 24 h. After 24 h of incubation, the culture medium was centrifuged (2000 *g*, 5 min) and the pellet was resuspended in 3 mL of BMMY medium (consisting of 1 % Yeast extract, 2 % peptone, 100 mM Potassium phosphate buffer pH 6.0, 0.34 % Yeast Nitrogen Base w/o amino acid and ammonium sulfate, 1 % ammonium sulfate, 0.5 % methanol, 0.00004 % Biotin). Induction was carried out for 48 h. The optimally integrated clone was used for scale-up in shake flask cultures. The colony was inoculated into 3 mL of BMGY medium and grown at 30 °C for 24 h. The preculture was then pour into 50 mL of BMGY medium and grown at 30 °C until OD_{600} = 3.0. At this point, the culture medium was centrifuged (3000 *g*, 15 min) and the pellet was resuspended in 100 mL of BMMY medium. Induction was performed at 30 °C for 48 h. Methanol was added to the culture every 24 h (final concentration of 0.5 % v/v).

The culture supernatant was recovered by centrifugation and ammonium sulfate precipitation was performed to recover the secreted proteins. Ammonium sulfate was added gradually up to 80% saturation at 4 °C with stirring. The obtained pellet was resuspended in 20 mM 2-(N-morpholino) ethanesulfonic acid (MES) buffer pH 6.5 and the ammonium sulfate was then removed by dialyzing 3 times. And the crude protein was loaded onto an anion exchange column and positive fractions were eluted with elution buffer (20 mM MES pH 6.5, 500 mM NaCl). Active fractions were confirmed by a 96-well plate enzyme activity assay (f.c. 0.6 mM PMS, 0.06 mM DCIP, 20 mM glucose) and were

dialyzed against 20 mM MES at 4 °C. Subsequently, the sample were subjected to the size exclusion chromatography, using the Superdex 200 Increase 10/300 GL columns (GE healthcare, USA). Fractions were eluted with buffer (20 mM MES pH 6.5, 100 mM NaCl). The enzymatic activity of the eluted fractions were analyzed by a 96-well plate enzyme activity assay, and active fractions were dialyzed against 20 mM MES at 4 °C. The purified enzyme obtained by this process was used for further evaluation.

2.4. Enzyme deglycosylation and SDS-PAGE analysis

Purified enzyme samples were subjected to SDS-PAGE analysis before and after deglycosylation. Deglycosylation of enzyme samples was carried out by mixing with denaturation buffer (Endo H deglycosylation kit) and incubated at 95 °C for 10 min. The denaturated enzymes were mixed with Endo H and incubated at 37 °C, for 1 h.

The molecular weight of deglycosylated enzymes and intact glycosylated enzymes were confirmed by SDS-PAGE analysis. The predicted molecular weight of designer FADGDH is 83 kDa and of AfGDH is 60 kDa.

2.5. Enzyme activity assay

Protein concentrations were measured using a DC protein assay kit (Bio-Rad, California, USA). Enzyme dehydrogenase activity towards glucose was determined using a PMS/DCIP activity assay (Sode et al., 2017). After mixing with the purified enzyme solution (f.c. 0.6 mM PMS and f.c. 0.06 mM DCIP), the reaction was initiated by the addition of glucose. We then calculated the activity by monitoring the decrease of DCIP absorbance at 600 nm. The reduction of 1 μmol DCIP in 1 min was defined as 1 unit of dehydrogenase activity, which corresponded to the oxidation of 1 μmol of glucose.

To evaluate the substrate specificity of designer FADGDH, the specific activity was determined using several saccharides (5 mM) using PMS/DCIP as the electron acceptors and compared with that toward a 5 mM glucose. The relative specific activity was defined as shown in the following equation.

$$\text{Relative specific activity} = \frac{Specific\ activity\ towardf\ .\ c.\quad 5\quad mM\ substrate}{Specfic\ activity\ towardf\ .\ c.\quad 5\quad mM\ glucose}$$

2.6. Absorption spectrum analysis

The transfer of electrons from FAD to heme could be observed by a spectrum change. The reaction mixture contained purified designer enzyme in 20 mM MES buffer (pH 6.5), and the electron transfer reaction was started by adding glucose. The absorption spectra were recorded using a V630 UV–VIS spectrophotometer (JASCO CO., Ltd., Tokyo, Japan) at 5 min, 10 min, 30 min, 60 min, 90 min, 120 min, and 180 min (measuring range: 400–600 nm). To analyze the effect of buffer pH and divalent cation ions on electron transfer, the buffer was replaced with 20 mM MES buffer (pH 6.0) via dialysis. The reaction mixture for evaluating the ion effect contained divalent cation ion solutions (f.c. 5 mM $CaCl_2$, f.c. 5 mM $MgCl_2$ or f.c. 5 mM $SrCl_2$) in 20 mM MES (pH 6.0). The spectra were recorded at 5 min, 10 min, 20 min, 30 min, 40 min, 50 min and 60 min (measuring range: 400–600 nm). The spectrum changing ratio was determined as the proportion of the reduction of heme at a certain time point compared to the total reduction of heme over the entire time course.

$$\text{Ratio} = \frac{\Delta Abs}{Abs_{50\ \ min}} \times \frac{1}{Time\quad (\text{min})}$$

2.7. Electrode preparation

To cover the electrode surface, a 0.2% multiwalled carbon nanotube solution was spotted onto SPCE sensor strips and dried at room temperature. Pyrenebutyric acid N-hydroxysuccinimide ester (PyNHS) was used as a linker for enzyme modification; 10 mM PyNHS was dissolved in N,N-dimethylformamide (DMF), spotted onto MWNT-SPCE and allowed to dry at room temperature. Purified PcCDH heme-AfGDH was immobilized on the electrode surface by an amine-coupling reaction. Enzyme solution was then spotted onto the PyNHS-MWNT-SPCE and incubated for 2 h at 25 °C. After the incubation, the electrodes were dried at room temperature, and stored in the dry cabinet until use. The enzyme-modified electrodes were used as the working electrodes in the following electrochemical analyses.

2.8. Electrochemical measurements

To confirm the direct electron transfer between the electron transfer domain of FADGDH and the electrode, chronoamperometry was performed using the following conditions: potential + 400 mV vs. Ag/AgCl, duration of 5 min/concentration, enzyme-modified electrode as the working electrode, Pt wire as the current electrode, Ag/AgCl as the reference electrode, cell volume 2.0 mL, temperature 25 °C, stirring 300 rpm. Prior to measurement, equilibration was performed in 100 mM P.P.B (pH 7.5 or 6.0) for 20 min. The measurement results were recorded using a PG580RM electrochemical analyzer (Uniscan Instruments, U.K.). Chronoamperometry was carried out in 100 mM potassium phosphate buffer (pH 6.0).

3. Results

3.1. Design of the engineered FADGDH harboring the P. chrisosporium CDH-derived heme b-binding cytochrome domain

First, the structural comparison between AfGDH and CDHs was carried out. Although the overall primary structural homology was low (22.2 %), the FAD binding region (1–571 for AfGDH, 229–773 for PcCDH, and 230–807 for MtCDH) and the catalytic residues (His505 and His548 for AfGDH, His706 and Asn749 for PcCDH, and His701 and Asn748 for MtCDH) are well conserved. Remarkably, the secondary structures as well as their FAD binding domains and C-terminal catalytic domains are also well conserved (Supplemental Fig. S1). AfGDHs (18 helices, 20 β strands) consist of two major domains. The FAD-binding domain includes a three-layer (β3 β5 α3) sandwich structure with eight short α helices, an irregular β sheet, and a long loop containing a short antiparallel β sheet. The C-terminal catalytic domain contains a large six-stranded antiparallel β sheet surrounded by six α helices and an additional short α helix. The flavin domains of PcCDH (28 helixes, 18 β strands) and MtCDH (23 helixes, 21 β strands) consist of two major domains. The FAD-binding domains of both PcCDH and MtCDH include a three-layer (β_2 β_5 α_4) sandwich structure with nine short α helixes (for PtCDH) or ten α helixes (for MtCDH), an irregular β sheet, and a long loop containing a short antiparallel β sheet. The C-terminal domains contain a large six-stranded antiparallel β sheet (for PtCDH) or a seven-stranded antiparallel β sheet (for MtCDH), surrounded by nine α helixes (PtCDH) or seven α helixes (MtCDH). Therefore, AfGDH and the FAD-binding domains of the two CDHs are structurally very similar molecules.

Fig. 1 shows a comparison of the 3D structures of AfGDH (PDB: 4YNU; Fig. 1a), and the full-length *Myriococcum thermophilum*-derived CDH (MtCDH), comprising a FAD-binding dehydrogenase domain and a heme *b*-binding cytochrome domain (PDB: 4QI6; Fig. 1b). Fig. 1 indicates that the wide open surfaces substrate accessing pockets of these molecules are very similar in structure, and this region is in the proximity of FAD. MtCDH harbors an additional domain, a heme *b*-binding cytochrome domain which is connected via a linker region consisted of 28 amino acids. This linker region connects the C-terminal region of a heme *b*-binding cytochrome domain in the distance of approximately 61.5 Å, to the N-terminal region of catalytic domain.

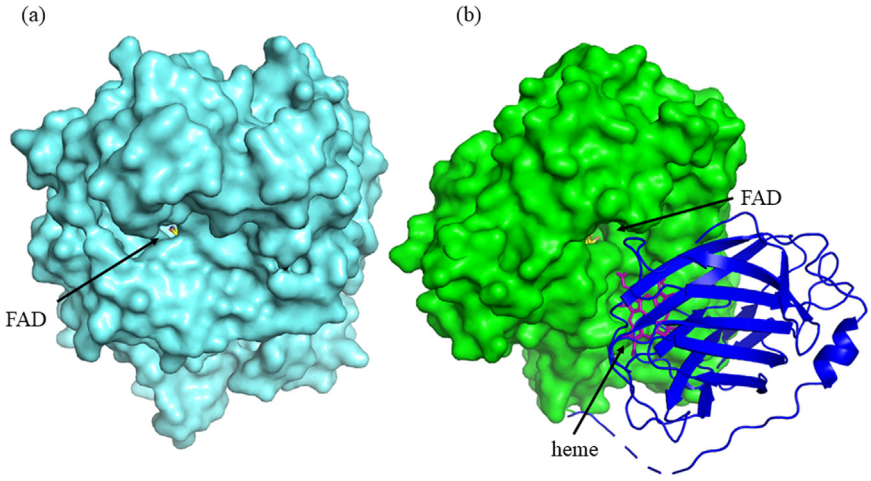

Fig. 1. Structural comparison of substrate accessing pocket between AfGDH (PDB:4YNU) (a) and Myryococcum thermophilum CDH (PDB:4QI6) (b) FAD is shown in yellow and heme is shown in purple. Heme *b*-binding cytochrome domain of MtCDH is shown as a blue ribbon structure. (For interpretation of the references to color in this figure legend, the reader is referred to the web version of this article.).

Remarkably, the heme *b*-binding cytochrome domain lies in the proximity of FAD at the substrate accessing pocket. In line with previous reports (Tan et al., 2015) of the CDH conformation needed to enable flavin-to-heme interdomain electron transfer, the heme molecule was within this distance—the heme molecule of the heme *b*-binding domain was 12.3 Å from FAD (N5) (Supplemental Fig. S2).

Fig. 2 shows the superimposition of AfGDH and full-length MtCDH. Interestingly, the heme molecules of the heme *b*-binding domain are proximal to FAD (N5) for both the MtCDH FAD-binding domain and AfGDH (Supplemental Fig. S2). Considering that the distance where direct electron transfer will occur is in the range of 15–30 Å (Stuchebrukhov, 2010), these observations inspired us to design a fusion enzyme molecule between AfGDH and the CDH-derived heme *b*-binding domain. The N-terminal region of AfGDH (blue dot-line circle) faces the substrate accessing side, similar to as those of the CDHs, whereas the C-terminal region of AfGDH (red dot-line circle) faces the opposite direction as those of the N-terminal structure. These structural observations enabled us to design an engineered AfGDH capable of DET by fusing the CDH-derived heme*b*-binding domain in its N-terminal region. Accordingly, the structural gene for the designer FADGDH with expected DET capabilities was constructed (Supplemental Fig. S3). The DNA fragment encoded a 215-amino-acid heme *b*-binding domain derived from PcCDH, with its original C-terminal native linker sequence but without its N-terminus signal sequence and was in-frame fused with the N-terminal region of the gene encoding a protein with 571 amino acids without a putative signal sequence. This designed and constructed gene, encoding the designer FADGDH, was inserted into the expression vector for integration into *Pichia pastoris*. The integrated gene was expressed using the alpha factor signal peptide sequence for secretion.

3.2. Enzymatic characterization of designer FADGDH

Fig. 3 shows the SDS-PAGE analysis of the designer FADGDH recombinantly prepared using *P. pastoris* as the host organism. The purified fraction derived from the culture supernatant of the recombinant *P. pastoris* expressing the designer FADGDH contained a smear band with a migration of larger than 130 kDa (lane 3), which was not observed in the non-transformant. Similarly, the purified fraction derived

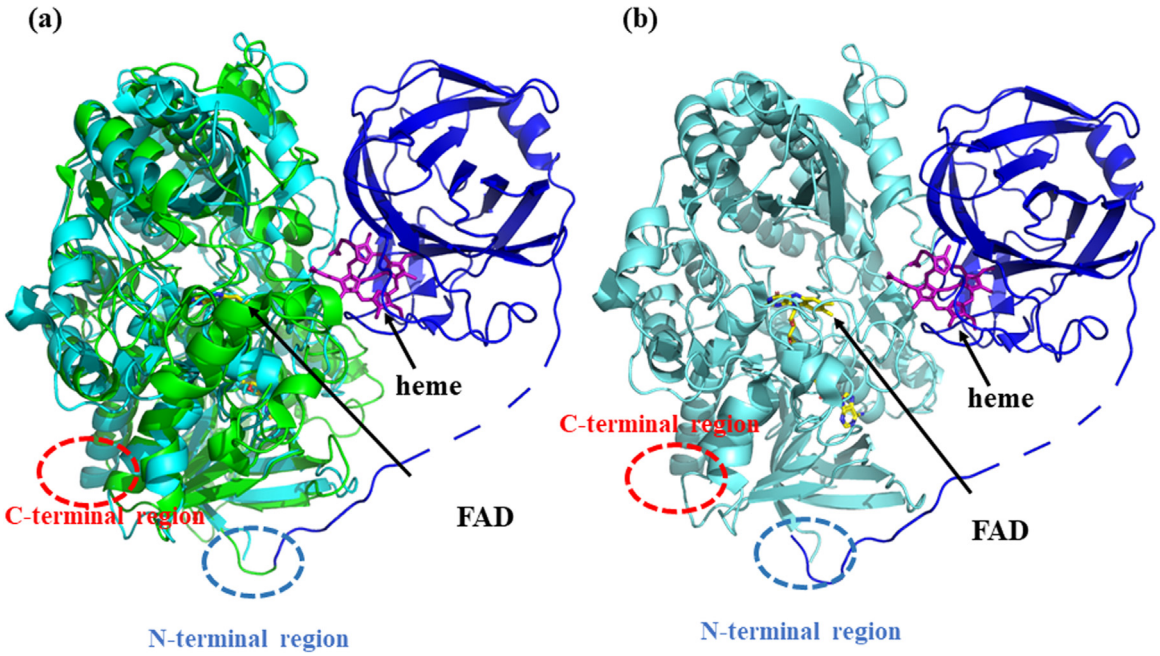

Fig. 2. Superimposition between AfGDH and MtCDH (a), and model structure of designer FADGDH (b) FAD is shown in yellow and heme is shown in purple. C-terminal region of AfGDH and MtCDH catalytic domain are shown in red circles and N-terminal regions were shown in blue circles. (For interpretation of the references to color in this figure legend, the reader is referred to the web version of this article.)

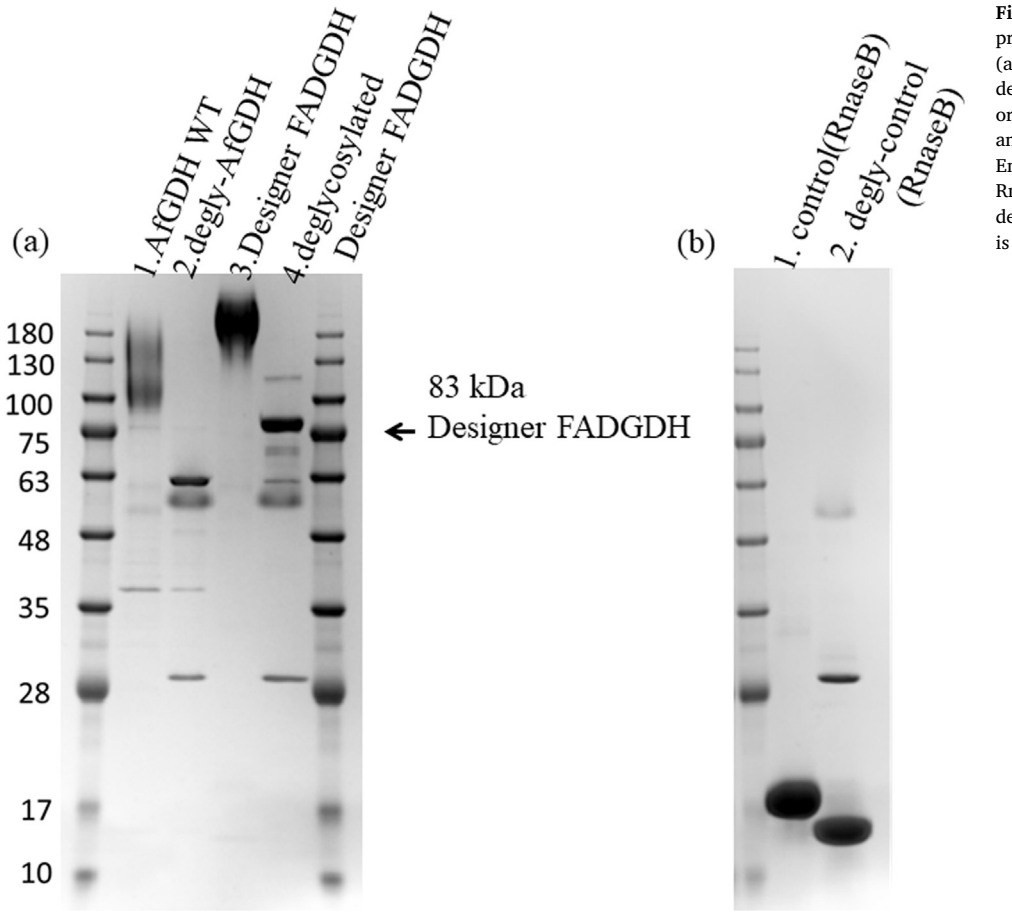

Fig. 3. SDSPAGE analyses of recombinantly produced designer FADGDH.
(a)SDSPAGE analyses of AfGDH (lane 1, 2) and designer FADGDH (lane 3, 4), before (lane1, 3) or after (2, 4) deglycosylation. (b)SDSPAGE analyses of RnaseB purchased from New England Biolabs (lane 1) and deglycosylated RnaseB (lane2). Predicted molecular weight of designer FADGDH is 83 kDa and of AfGDH WT is 60 kDa, in their non-glycosylated forms.

from the culture supernatant of the recombinant *P. pastoris* expressing the AfGDH contained a smear band with a migration of larger than 100 kDa (lane 1). These results suggested these recombinant products excreted in the culture were glycosylated. Therefore, these purified fractions were deglycosylated, and subjected to the SDSPAGE analyses. The deglycosylated fraction derived from the culture supernatant of the recombinant *P. pastoris* expressing the designer FADGDH contained a clear band with a migration of 83 kDa (lane 4), which is the expected gene product of designer FADGDH. In contrary, the deglycosylated fraction derived from the culture supernatant of the recombinant *P. pastoris* expressing the AfGDH contained a clear band with a migration of 62 kDa (lane 2), which is the expected gene product of AfGDH. These results suggest that the designer FADGDH was secretionally expressed as a soluble, active and glycosylated protein by recombinant *P. pastoris*, with a different molecular weight from that of wild-type AfGDH.

This purified protein sample was then analyzed for dye-mediated glucose dehydrogenase activity using PMS/DCIP as the electron acceptor (Table 1). The V_{max} value of the purified sample with PMS/DCIP towards glucose was 250 U/mg, with a K_m value of 53 mM. The value was slightly lower than that of the wild-type AfGDH (V_{max} = 340 U/mg, K_m = 39 mM).

Table 1
Enzymatic activity of AfGDH wild type and designer FADGDH using PMS/DCIP (at 20 mM glucose concentration) as electron acceptors in a solution, measured spectrophotometrically.

	PMS/DCIP	
	V_{max} (U/mg)	K_m (mM)
AfGDH wild type	340	39
Designer FADGDH	250	53

These results show that the purified sample contained recombinant protein that had dye-mediated glucose dehydrogenase activity similar to that of wild-type AfGDH. Substrate specificity of designer FADGDH was also investigated (Supplemental Fig. S4), revealing the identical substrate specificity with the parental AfGDH. Therefore, the addition of N-terminal heme *b*-binding cytochrome domain of CDH to AfGDH did not result any alteration in the reductive half reaction of parental enzyme. In addition oxidase activity was also investigated. The experiments were carried out with the air-saturated sample solution containing glucose, in the presence or absence of electron acceptor. In the absence of electron acceptor, but by the presence of enough dissolved oxygen, the designer FADGDH did not liberate any detectable hydrogen peroxide, similar as AfGDH, confirming that designer FADGDH did not show oxidase activity.

To investigate the electron transfer from FAD to the fused heme *b*-binding cytochrome domain of CDH in this sample, spectroscopic observation was carried out. Fig. 4a shows the differential spectra before and after the addition of glucose in the sample solution of pH 6.5 MES buffer. Before the addition of glucose, a significant absorption spectrum was observed at 432 nm, corresponding to Soret band of the heme. The addition of glucose resulted in a drastic increase of the absorption spectrum at 532 nm and 562 nm, which are the typical absorption spectra of reduced heme. These results clearly indicated that the recombinantly produced and purified designer FADGDH sample had dye-mediated glucose dehydrogenase activity and harbored the heme *b*-binding cytochrome domain, as designed. Moreover, the reduced FAD formed by the oxidation of glucose could transfer electrons to the N-terminally fused heme *b*-binding cytochrome domain, resulting in its reduced heme form. In other words, the intramolecular electron transfer between FAD and heme was confirmed, as expected, in the

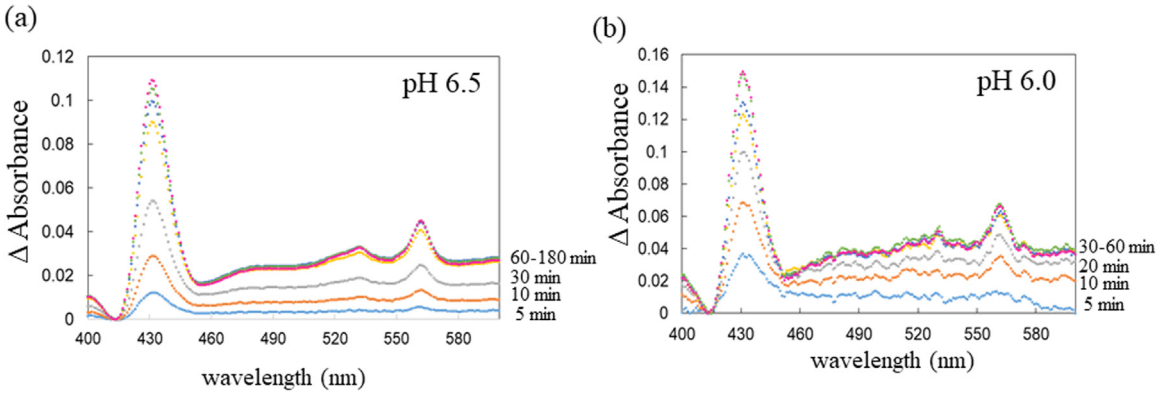

Fig. 4. Differential spectra of designer FADGDH at pH 6.5 (a) and pH 6.0 (b).
(a)Absorbance was plotted at 0–180 min (SkyBlue; 5 min, Orange; 10 min, Gray; 30 min, Yellow; 60 min, Dark Blue; 90 min, Light Green; 120 min, Red; 180 min). (b) Absorbance was plotted at 0–60 min (SkyBlue; 5 min, Orange; 10 min, Gray; 20 min, Yellow; 30 min, Blue; 40 min, Light Green; 50 min, Red; 60 min) Absorbance at the wavelength of 432 nm was ascribed to Soret band, and 532 nm and 562 nm was ascribed to reduced heme. (For interpretation of the references to color in this figure legend, the reader is referred to the web version of this article.).

designer FADGDH.

The impact of pH and the presence of different cations in the intramolecular electron transfer of the designer FADGDH was then investigated. Fig. 4b shows the differential spectra before and after the addition of glucose in the sample solution of pH 6.0 MES buffer. Similar to the results at pH 6.5 (Fig. 4a), the addition of glucose resulted the shift of the Soret band and an increase of the absorption spectrum at 532 nm and 562 nm. The change of pH from pH 6.5 to pH 6.0 resulted in the increase of the relative heme reducing speed by 2.6 fold (from 3.9/min at pH 6.5 to 10.3/min at pH 6.0). Figs. 5a and 5b show the impact of the presence of different divalent cations on the reduction of heme by the designer FADGDH in the presence of glucose by measuring the relative absorption change at either 432 nm (Fig. 5a) or 562 nm (Fig. 5b) using MES buffer at pH 6.0. The electron transfer rate increased by approximately 2 times in the presence of 5 mM Ca^{2+} or Sr^{2+} in the solution. These results indicate that the mechanisms of intramolecular electron transfer might be similar to those observed in CDH and indicate strategies to further improve the electron transfer efficiency of the designer FADGDH.

3.3. Electrochemical characterization of designer FADGDH

To evaluate the DET ability of the designer FADGDH between the enzyme and electrode, electrochemical analysis was performed using enzyme-modified SPCE as a working electrode. Although the enzyme electrode with immobilized wild-type AfGDH without a heme domain did not show a current increase by the addition of glucose (Hatada et al., 2018), the enzyme electrode with immobilized designer FADGDH did show a current increase immediately after the addition of glucose to the sample solution, as shown in Fig. 6a. This indicated that the reduced heme *b*-binding cytochrome domain of the designer FADGDH, which was formed by the oxidation of glucose, was immediately oxidized on the electrode, thereby showing DET reaction with the electrode. By scanning oxidation potential, the dependency of current response on applied potential was also investigated (Supplemental Fig. S5). Current increase was observed from even at 0 mV vs Ag/AgCl, and more obvious at 200 mV vs Ag/AgCl, however clear difference was observed at higher potential, therefore, further investigation was carried out at 400 mV. The Fig. 6b shows the correlation between the glucose concentration and the observed current increase. The current increase showed glucose concentration dependency (Fig. 6b). However, the response toward the first glucose sample addition was more obvious than further successive glucose sample addition (Fig. 6c). Considering that the current increase toward the glucose addition was immediately observed, indicating DET reaction was rapid, the reduction of heme *b* would be the rate limiting step.

Hence, it was confirmed that the designer FADGDH was recombinantly prepared as the fusion molecule of FADGDH and the heme

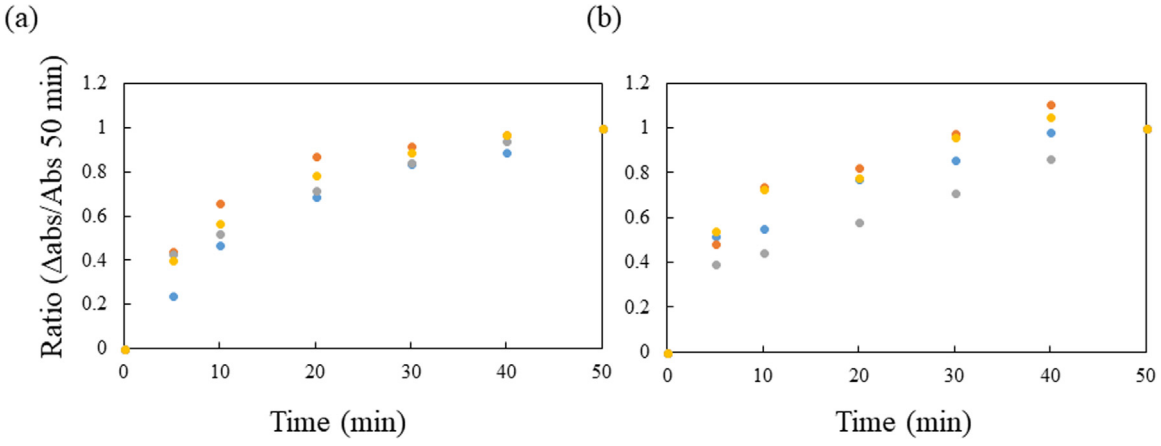

Fig. 5. Time course of differential spectrum increase in the presence of divalent cations. Differential spectra of designer FADGDH in 20 mM MES buffer (pH 6.0) at 432 nm (a) or 562 nm (b) are shown. The increased absorbance was plotted from 0 to 60 min (Blue; without divalent cation, Orange; containing 5 mM $CaCl_2$, Gray; containing 5 mM $MgCl_2$, Yellow; containing 5 mM $SrCl_2$). (For interpretation of the references to color in this figure legend, the reader is referred to the web version of this article.).

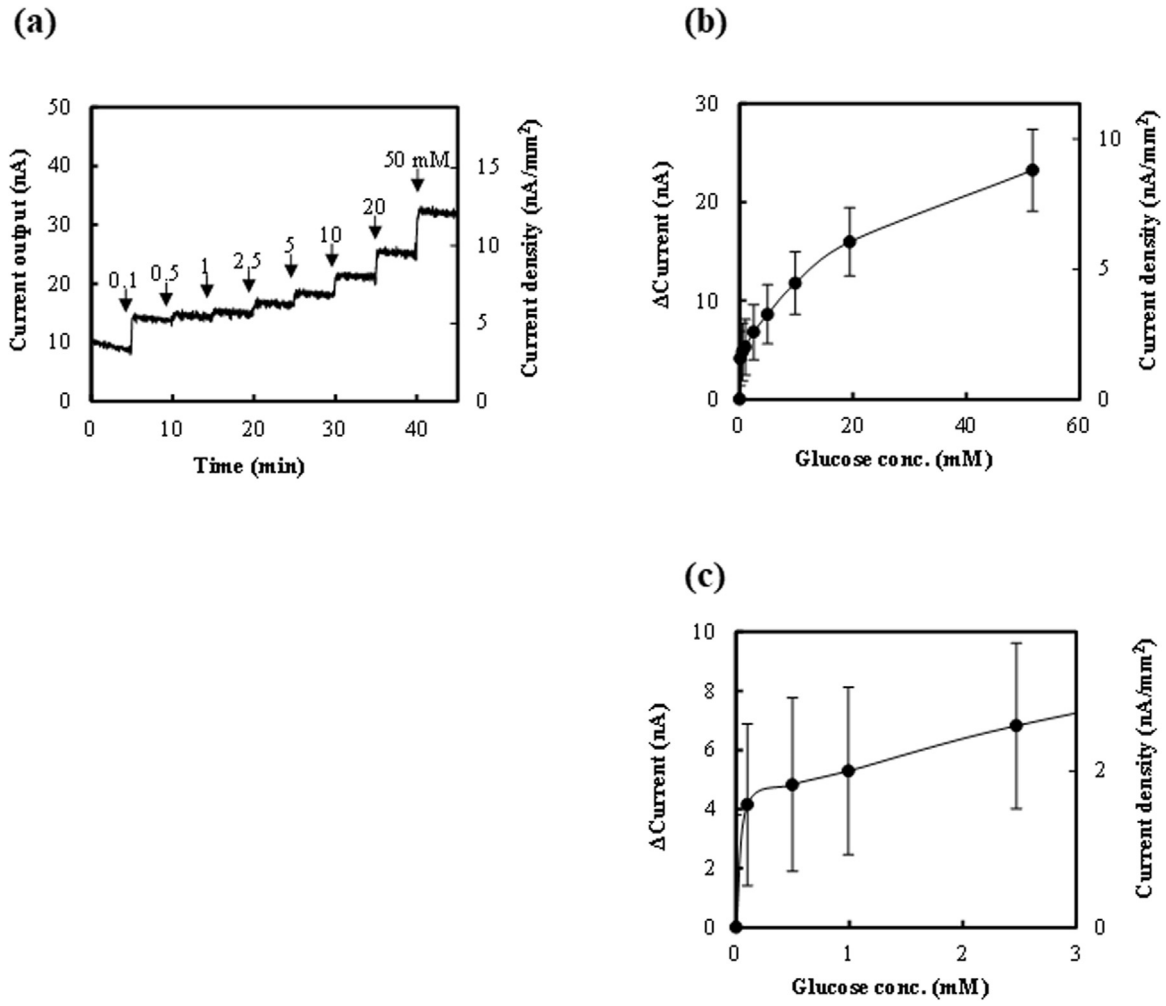

Fig. 6. Chronoamperometric analysis of the electrode with immobilized designer FADGDH. (a) The response curve of the electrode with immobilized designer FADGDH upon the addition of glucose by applying + 400 mV vs Ag/AgCl. The arrows indicate the times at which glucose was added, with the final glucose concentrations (mM). Noise reduction was performed on the chronoamperometry data using moving average filtration. (b) The correlation between the glucose concentration and the current increase (n = 2). (c) The expansion of b at glucose concentration from 0 to 3 mM.

b-binding cytochrome domain, and it possessed unique dye-mediated glucose dehydrogenase activity, showing the intramolecular electron transfer between FAD and heme. Furthermore, the heme showed DET ability. Therefore, the designer FADGDH is confirmed as a novel GDH, possessing electrode DET ability.

4. Discussion

In this study, a designer FADGDH was constructed by fusing a representative fungal FADGDH and a CDH-derived heme *b*-binding cytochrome domain, aiming to develop a novel FADGDH for CGM that is capable of direct electron transfer with the electrode. The original concept of this approach was based on the elucidated structural similarity of FADGDH and the CDH flavin catalytic domain and the observations of the superimposition of FADGDH and the entire CDH. In addition, our recent development of a glucose sensor that employs a quick and easy modification method with a mediator suggested that the modification of a non-DET enzyme surface with the appropriate electron acceptor, in proximity to where FAD can transfer electrons directly, may transform a non-DET enzyme into a DET enzyme. Considering the results of the superimposition of FADGDH and the entire CDH, the heme in the CDH-derived heme *b*-binding cytochrome domain may exist in proximity to the FAD of AfGDH when the CDH-derived heme *b*-binding cytochrome domain is fused to the AfGDH N-terminal region. Therefore, intramolecular electron transfer will be achieved between FAD and heme, consequently enabling the DET.

To prepare this designer FADGDH the most popular host microorganism, *Escherichia coli*, could not be utilized. The majority of FAD-harboring oxidoreductases are produced and folded in the cytosol in Gram-negative bacteria, whereas heme *b*- and heme *c*-containing electron transfer molecules are produced as unfolded molecules in the cytosol. They are then transferred to the periplasmic space by Sec secretory machinery, where they are subjected to post-translational modifications that either non-covalently bind heme to form heme *b* or covalently bind heme to form heme *c*. The designer FADGDH is composed of two domains that would normally be folded and matured via different post-translational pathways; however, the molecule is transcribed and translated in-frame and is fused as one protein molecule. Therefore, the designer FADGDH could not be produced in *E. coli*. In contrast, the yeast *P. pastoris*, has been reported to produce fully functional CDH, having similar structure as designer FADGDH. Therefore, we selected *P. pastoris* to recombinantly produce designer FADGDH as the host organism.

As a result, designer FADGDH was produced as a soluble bifunctional enzyme molecule, showing both FADGDH catalytic activity and heme *b*-like redox properties. Spectroscopic observations clearly showed that the designer FADGDH could carry out the intramolecular electron transfer between FAD and heme, which was confirmed by the

reduced heme-specific spectra that were observed upon the addition of glucose. Interestingly, lowering the pH from pH 6.5 to pH 6.0 and/or the presence of divalent cations resulted in an increase in the rate of reduction of heme. Alterations in the intramolecular electron transfer efficiency of CDH have been evaluated and reported by several researchers. Igarashi et al. (2002, 2005) reported the pH dependency of the intramolecular electron transfer ability. The impact of the presence of divalent cations on the CDH intramolecular electron transfer ability was also investigated (Kadek et al., 2015; Kracher et al., 2015), and Ca^{2+} was reported to be the most effective ion for the improvement of interelectron transfer activity. Kracher et al. (2015) elucidated the 3D crystal structure and showed the ability of divalent cations to reduce the surface electron repulsion between the domain interfaces. In addition, Kadek et al.m(2017) analyzed the correlation of the pH and the protein surface electrostatics, which was consistent with the observation that both lowering the pH and the presence of divalent cations increased the rate of intramolecular electron transfer between FAD and heme by reducing the surface electron repulsion of the interface. Therefore, the observed increased intramolecular electron transfer ratio in the designer FADGDH might also be caused by the alteration of the surface charge at the residues which compose the interface region of each domain. Although the intramolecular electron transfer ability of the designer FADGDH increased by lowering the pH, the speed was lower than that of CDH. In addition, the addition of divalent cations also improved the intramolecular electron transfer of the designer FADGDH. These observations suggest that a decrease in pH and the addition of divalent cations might affect electron repulsion at the domain interface, thereby improving the intramolecular electron transfer of the designer FADGDH. However, considering that the speed was lower than that of CDH, the region in AfGDH where the heme *b*-binding cytochrome domain may interact may have a different charge distribution from that of the CDH catalytic domain.

As shown in Fig. 6, the designer FADGDH showed DET ability at the electrode. This was not observed from the electrode with immobilized wild-type AfGDH, which does not harbor an electron transfer domain. There are numerous reports showing the DET ability of the CDH-derived heme *b*-binding cytochrome domain. The rapid current increase observed in the DET-dependent electrochemical reaction confirmed that the fully active DET property of the in-frame-fused CDH-derived heme *b*-binding cytochrome domain in the N-terminal region of AfGDH was retained and expressed. Namely, the structural flexibility of the N-terminal-fused CDH-derived heme *b*-binding cytochrome domain was retained to make possible its function as the shuttle between FAD and the electrode. However, there are two significant observations to understand concerning the improvement of the DET properties of the designer FADGDH. First, the glucose concentration-dependent current increase from the DET reaction was more sensitive at the first glucose sample addition, than other successive glucose sample additions. Considering that the designer FADGDH retained similar catalytic activity toward glucose as the original enzyme, and also DET reaction of heme *b* cytochrome domain was very rapid, this observation suggested that slow intra-molecular electron transfer prevents proportional current increase with increasing glucose concentration. In addition, the observed apparent K_m value calculated from the correlation of glucose concentration and DET derived catalytic current in Fig. 6b was far lower (K_{mapp} = 8.6 mM) than those obtained from the catalytic reaction in the solution using electron acceptors (K_m = 53 mM). Considering that no significant change was observed in the catalytic properties of designer FADGDH compared with parental AfGDH, the observed decreased K_{mapp} value might be due to the limitation of the availability in the electron acceptor in the oxidative half reaction in the DET experiment. Second, there was a slow progression of heme reduction. The dye-mediated dehydrogenase activity investigated using PMS/DCIP as the electron acceptor revealed no significant alteration in its catalytic activity for glucose oxidation. In addition, the decrease in pH as well as the addition of divalent cations affected intra-molecular electron transfer efficiency. Therefore, these observations suggest that the rate limiting step of the DET-based electrochemical reaction was not the reductive half reaction at the FAD dehydrogenase “catalytic domain”, nor the DET reaction of heme with the electrode, but occurred at the intramolecular electron transfer between FAD and heme. Considering that the interaction between the catalytic domain and the electron transfer domains of CDH are regulated by electro-repulsion/attraction forces at the domains’ interface, the investigation of the effect of pH and the presence of divalent cations on intramolecular electron transfer suggests that the interaction of the domains in the designer FADGDH is different from that of CDH. The insufficient affinity between the regions in AfGDH where the heme *b*-binding cytochrome domain may interact might result in this unfavorable, slow intramolecular electron transfer between FAD and heme, consequently causing the narrow dynamic range in the glucose concentration-dependent current increase of the DET-based electrochemical reaction.

To obtain more detailed structural evidence to support our aforementioned assumption, the surface electrostatic potentials of the AfGDH, catalytic domain of PcCDH, and the heme *b*-binding cytochrome domain of PcCDH were evaluated using Adaptive Poisson-Boltzmann Solver software, as shown in Fig. 7. The heme *b*-binding cytochrome domain was primarily negatively charged (shown in red) at both pH values (Fig. 7e and f). The surface charge of the CDH catalytic domain was obviously changed by the pH (Figs. 7c and 7d), by increasing blue dots at pH5.5, representing positively charged residues. Mainly neutral to positively charged residues were observed at pH 7.5, whereas the positively charged residues were significantly increased at pH 5.5, especially in the predicted internal region where the heme *b*-binding cytochrome domain may interact, which were indicated by yellow dot circles. The surface charge of AfGDH at pH 7.5 was more negative (Fig. 7b), and positively charged residues increased at the rim of the predicted region where the heme *b*-binding cytochrome domain may interact (indicated by yellow dot circles); however, the internal residues remained negative at pH 5.5 (Fig. 7a). This difference, where the CDH catalytic domain changes charge from neutral to positive in the internal region when shifting the pH from pH 7.5 to 5.5 while the AfGDH remains positive in the internal region, might be the main reason why the intramolecular electron transfer is inferior to that of CDH. These relevant and consistent findings, based on the structural investigation and the comparison between experimental observations, will provide us with a novel strategic approach to improve the DET properties of the designer FADGDH. Namely, amino acid substitutions, that do not alter the structural and functional properties of AfGDH, at the residues where the neutral to positively charged amino acids interact with the negatively charged heme *b*-binding cytochrome domain will significantly improve the DET properties of the designer FADGDH.

5. Conclusion

In this study, a designer FADGDH was constructed to develop a novel FADGDH for CGM that is capable of direct electron transfer with an electrode. The superimposition of the FADGDH and CDH structures suggested that the heme in the CDH-derived heme *b*-binding cytochrome domain would be proximal to the FAD (N5) of AfGDH if the CDH-derived heme *b*-binding cytochrome domain was fused to the AfGDH N-terminal region. Consequently, AfGDH was selected as the catalytic domain and linked to a *Phanerochaete chrisosporium* CDH (PcCDH)-derived heme *b*-binding cytochrome domain with a native linker. The recombinant production of the designer FADGDH resulted in a soluble and active FADGDH, showing flavin-to-heme interdomain electron transfer during the oxidation of glucose. Most remarkably, this molecule showed DET ability to the electrode and maintained the original substrate specificity of FADGDH. In addition, the observed DET property suggested that the rate limiting step of the DET-based electrochemical reaction was not the reductive half reaction at the FAD dehydrogenase “catalytic domain”, nor the DET reaction of heme with

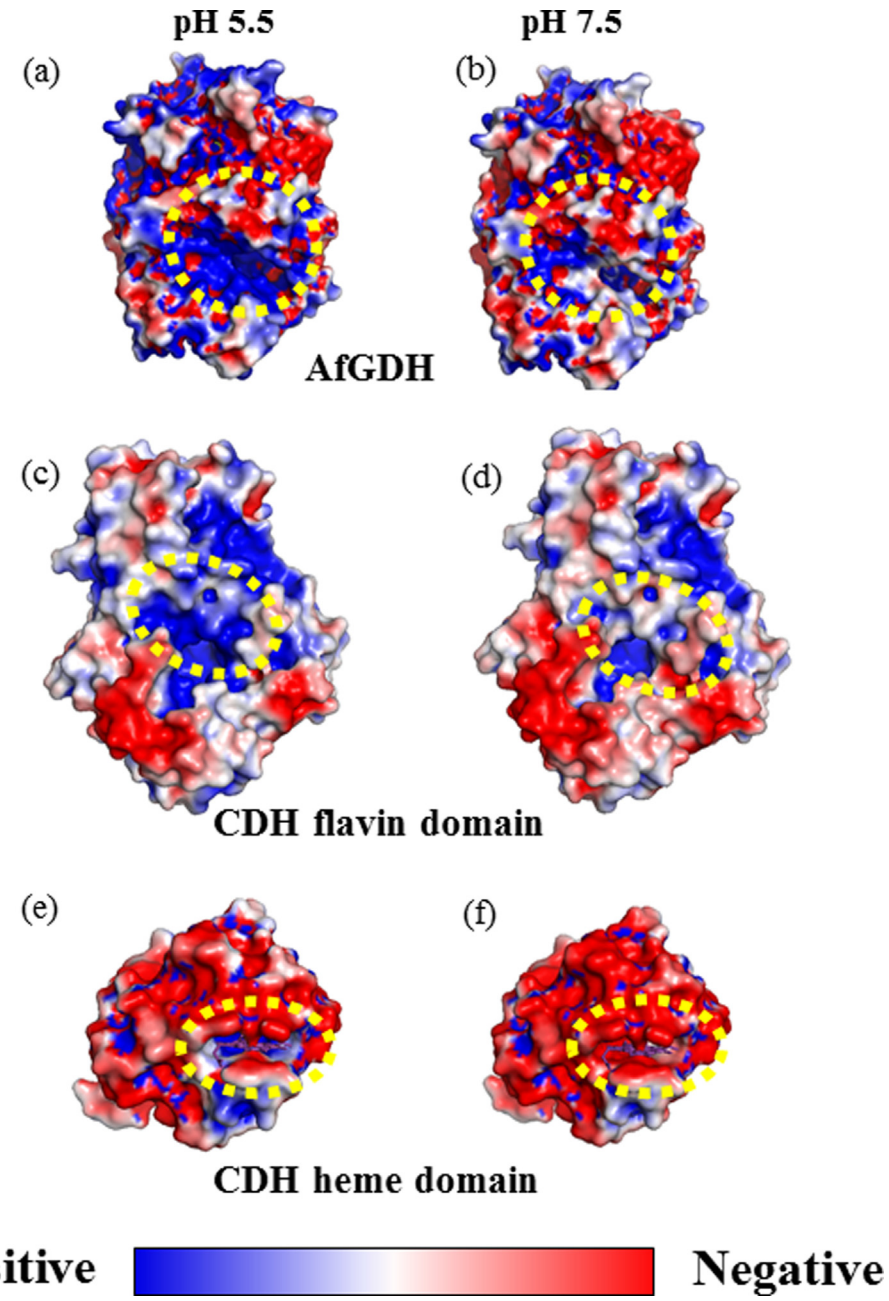

Fig. 7. The pH dependency of the surface electrostatic potentials of the AfGDH, catalytic domain and heme *b*-binding cytochrome domain of PcCDH. The surface electrostatic potentials were evaluated at pH 5.5 (a, c, e) or at pH 7.5 (b, d, f) using software of Adaptive Poisson-Boltzmann Solver. Protein surface electrostatics of AfGDH (Top) (a, b), catalytic domain (middle) (c, d) and electron transfer domain of PcCDH (bottom) (e, f) are shown. Potential charge is shown as color in red (negative), in blue (positive) or in gray (neutral). Yellow circles indicate the regions that potentially function as the interface between the catalytic domain and electron transfer domain. Color indicator suggested that the gradation in the molecular surface of red means more negative and blue means more positive. (For interpretation of the references to color in this figure legend, the reader is referred to the web version of this article.).

the electrode, but occurred at the intramolecular electron transfer between FAD and heme. The surface electrostatic potential predictions of the AfGDH catalytic domain and the heme *b*-binding cytochrome domain of PcCDH suggested the main reason why the intramolecular electron transfer of the designer FADGDH is inferior to that of CDH. These relevant and consistent findings, based on the structural investigation and the comparison between experimental observations, will provide us with a novel strategic approach to improve the DET properties of the designer FADGDH.

Acknowledgement

K. I. was supported by the Japan Student Services Organization (JASSO) and by the Precise Measurement Technique promoting foundation.

Appendix A. Supporting information

Supplementary data associated with this article can be found in the online version at doi:10.1016/j.bios.2018.07.027.

References

Bak, T.G., 1967a. Biochim. Biophys. Acta 139 (2), 277–293.
Bak, T.G., 1967b. Biochim. Biophys. Acta 146 (2), 317–327.
Bak, T.G., Sato, R., 1967a. Biochim. Biophys. Acta 139 (2), 265–276.
Bak, T.G., Sato, R., 1967b. Biochim. Biophys. Acta 146 (2), 328–335.
Bartlett, P.N., Al-Lolage, F.A., 2017. J. Electroanal. Chem. 819 (15), 26–37.
Desriani, Ferri, S., Sode, K., 2010. Biotechnol. Lett. 32 (6), 855–859.
Ferri, S., Kojima, K., Sode, K., 2011. J. Diabetes Sci. Technol. 5 (5), 1068–1076.
Hallberg, B.M., Bergfors, T., Bäckbro, K., Pettersson, G., Henriksson, G., Divne, C., 2000. Structure 8 (1), 79–88.
Hallberg, B.M., Henriksson, G., Pettersson, G., Divne, C., 2002. J. Mol. Biol. 315 (3), 421–434.
Harreither, W., Felice, A.K., Paukner, R., Gorton, L., Ludwig, R., Sygmund, C., 2012. Biotechnol. J. 7 (11), 1359–1366.
Hatada, M., Loew, N., Inose-Takahashi, Y., Okuda-Shimazaki, J., Tsugawa, W.,

Mulchandani, A., Sode, K., 2018. Bioelectrochemistry 121, 185–190.
Igarashi, K., Momohara, I., Nishino, T., Samejima, M., 2002. Biochem J. 365 (Pt 2), 521–526.
Igarashi, K., Yoshida, M., Matsumura, H., Nakamura, N., Ohno, H., Samejima, M., Nishino, T., 2005. FEBS J. 272 (11), 2869–2877.
Ito, H., Murata, K., Kimura, A., 1983. Agric. Biol. Chem. 47 (7), 1691–1692.
Kadek, A., Kavan, D., Felice, A.K., Ludwig, R., Halada, P., Man, P., 2015. FEBS Lett. 589 (11), 1194–1199.
Kadek, A., Kavan, D., Marcoux, J., Stojko, J., Felice, A.K., Cianférani, S., Ludwig, R., Halada, P., Man, P., 2017. Biochim. Biophys. Acta 1861 (2), 157–167.
Kracher, D., Zahma, K., Schulz, C., Sygmund, C., Gorton, L., Ludwig, R., 2015. FEBS J. 282 (16), 3136–3148.
Mori, K., Nakajima, M., Kojima, K., Murakami, K., Ferri, S., Sode, K., 2011. Biotechnol. Lett. 33 (11), 2255–2263.
Ogura, Y., Nagahisa, M., 1937. Bot. Mag. 597–612.
Ozawa, K., Iwasa, H., Sasaki, N., Kinoshita, N., Hiratsuka, A., Yokoyama, K., 2017. Appl. Microbiol. Biotechnol. 101 (1), 173–183.
Piumi, F., Levasseur, A., Navarro, D., Zhou, S., Mathieu, Y., Ropartz, D., Ludwig, R., Faulds, C.B., Record, E., 2014. Appl. Microbiol. Biotechnol. 98 (24), 10105–10118.
Satake, R., Ichiyanagi, A., Ichikawa, K., Hirokawa, K., Araki, Y., Yoshimura, T., Gomi, K., 2015. J. Biosci. Bioeng. 120 (5), 498–503.
Sode, K, Loew, N, Ohnishi, Y, Tsuruta, H, Mori, K, Kojima, K, Tsugawa, W, LaBelle, J.T., Klonoff, D.C., 2017. Biosens. Bioelectron. 87, 305–311.
Stuchebrukhov, A.A., 2010. Laser Phys. 20 (1), 125–138.
Sygmund, C., Klausberger, M., Felice, A.K., Ludwig, R., 2011a. Microbiology 157 (Pt 11), 3203–3212.
Sygmund, C., Staudigl, P., Klausberger, M., Pinotsis, N., Djinović-Carugo, K., Gorton, L., Haltrich, D., Ludwig, R., 2011b. Microb. Cell Fact. 10, 106.
Sygmund, C., Kracher, D., Scheiblbrandner, S., Zahma, K., Felice, A.K., Harreither, W., Kittl, R., Ludwig, R., 2012. Appl. Environ. Microbiol 78 (17), 6161–6171.
Tan, T.C., Kracher, D., Gandini, R., Sygmund, C., Kittl, R., Haltrich, D., Hällberg, B.M., Ludwig, R., Divne, C., 2015. Nat. Commun. 6, 7542.
Tsujimura, S., Kojima, S., Kano, K., Ikeda, T., Sato, M., Sanada, H., Omura, H., 2006. Biosci. Biotechnol. Biochem. 70 (3), 654–659.
Vogt, S., Schneider, M., Schaefer-Eberwein, H., Noell, G., 2014. Anal. Chem. 86, 7530–7535.
Wilson, G., 2016. Biosens. Bioelectron. 82, 7–8.
Yang, Y., Huang, L., Wang, J., Wang, X., Xu, Z., 2014. J. Microbiol. Biotechnol. 24 (11), 1516–1524.
Yang, Y., Huang, L., Wang, J., Xu, Z., 2015. Enzyme Microb. Technol. 68, 43–49.
Yoshida, H., Sakai, G., Mori, K., Kojima, K., Kamitori, S., Sode, K., 2015. Sci. Rep. 5, 13498.